

Figure S1. Immunohistology for fibrosis in lungs from MCTPN study using Picrosirius Red Stain. Representative photomicrograph of Picrosirius stain in vehicle (*A*) and seralutinib-treated group (*B*). Thin arrows point to pulmonary arteriole lumen. (*A*) Vehicle-treated animal showing extensive peri-vascular fibrosis (thick arrow). (*B*) Seralutinib-treated animal. Scale bars, 200µm.

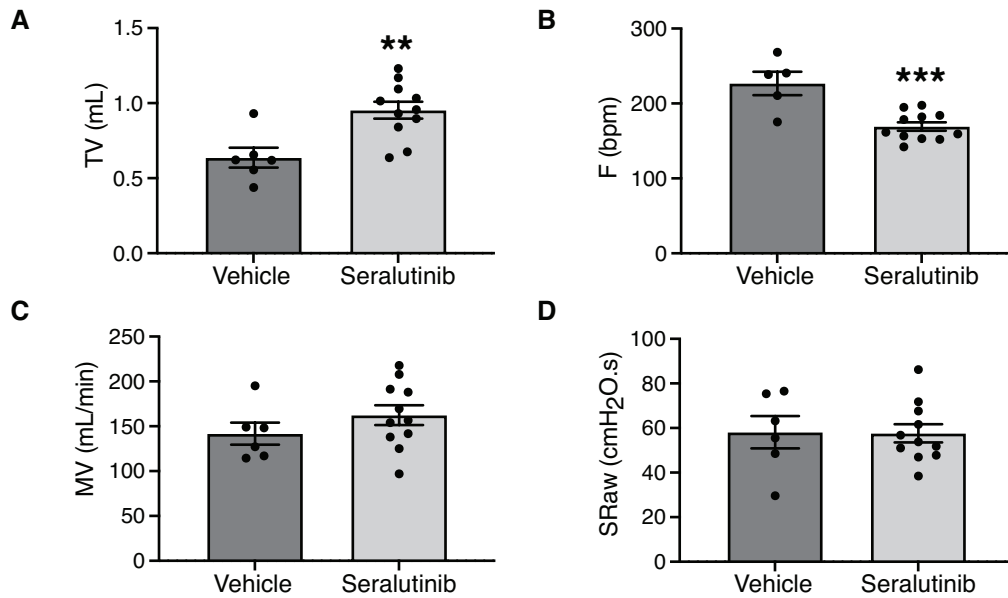


Figure S2. Effects of seralutinib on respiratory parameters in the monocrotaline pneumonectomy (MCTPN) model. Bar graphs show the effect of seralutinib (light grey) vs vehicle (dark grey) on (A) tidal volume (TV), (B) respiratory rate (F; bpm, breaths per minute), (C) minute ventilation (MV; milliliters per minute), and (D) airway resistance (S_{Raw}; cmH₂O.s). Data are shown as mean \pm standard error of the mean (SEM) (n= 6 for vehicle, n=11 for seralutinib). Statistical analysis was performed using unpaired t-test. **P<0.005, ***P<0.001 versus vehicle.

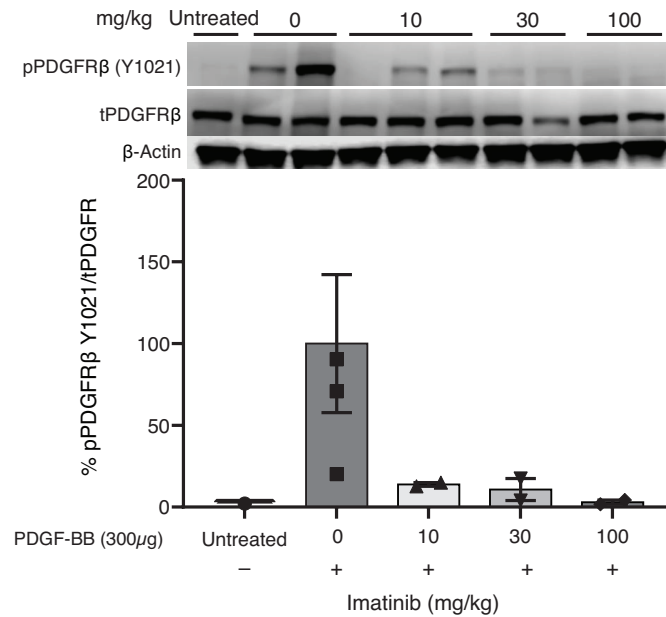


Figure S3. Imatinib in vivo pharmacodynamic (PD) profile. Male SD rats received vehicle (0 mg/kg) or imatinib 10mg/kg, 30mg/kg or 100mg/kg via oral gavage for two consecutive days. Rats were administered PDGF-BB via intratracheal insufflation into the lungs six hours post-dose. Five minutes post-challenge, lungs were harvested to measure phosphorylation of PDGFR. Data presented as percent change in phospho PDGFRβ (Y1021)/ total PDGFRβ by western blot analysis. Data presented as mean \pm standard error of the mean (SEM) (n=1 for Naïve, n=4 for Vehicle, n=2 for all imatinib doses).

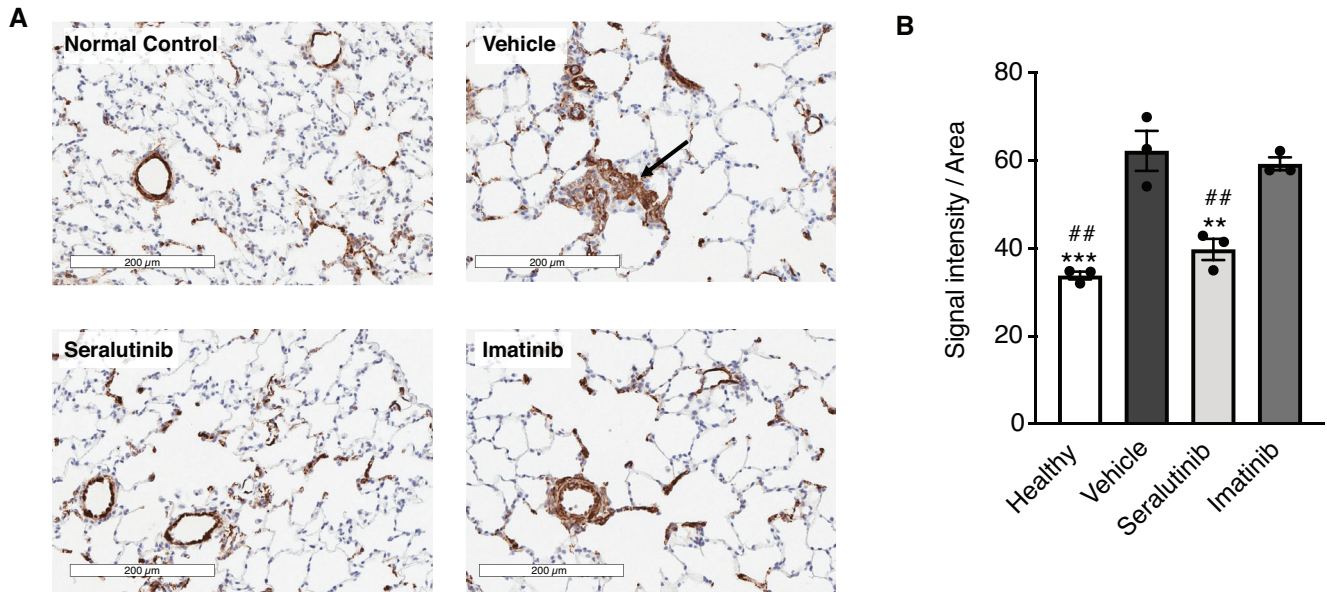


Figure S4. (A) Immunohistology of smooth muscle actin to visualize muscularization of pulmonary arteries in SU5416/H study. Representative images from normal, vehicle, seralutinib- and imatinib-treated lungs are shown. Arrow points to plexiform lesion in vehicle group. (B) Quantification of SMA stain. Data represents mean \pm standard error of the mean (SEM), n=3 for all groups. Statistical analysis was performed using one-way ANOVA with Dunnett's multiple comparisons test. **p<0.005, ***P<0.001 versus vehicle; ##p<0.01 versus imatinib. Scale bar, 200 μ m.

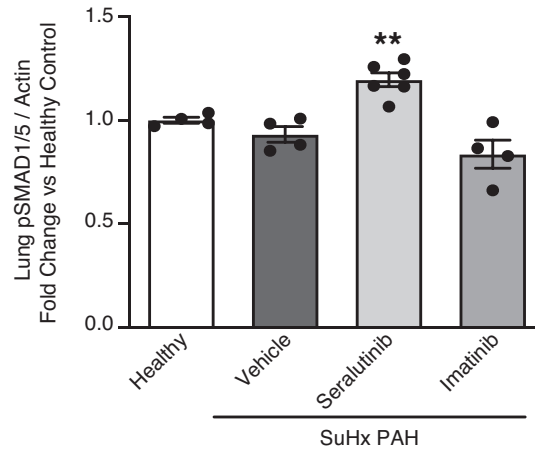


Figure S5. phospho-SMAD1/5 / β -Actin fold change in SU5416/H rat lungs relative to healthy controls at the end of the treatment period (day 49, Study 3). Data are presented as mean \pm standard error of the mean (SEM) for healthy (n=4), vehicle (n=4), serlutinib (n=6), imatinib (n=4). Statistical analysis was performed using one-way ANOVA with Dunnett's multiple comparisons test, **P<0.005 versus vehicle.

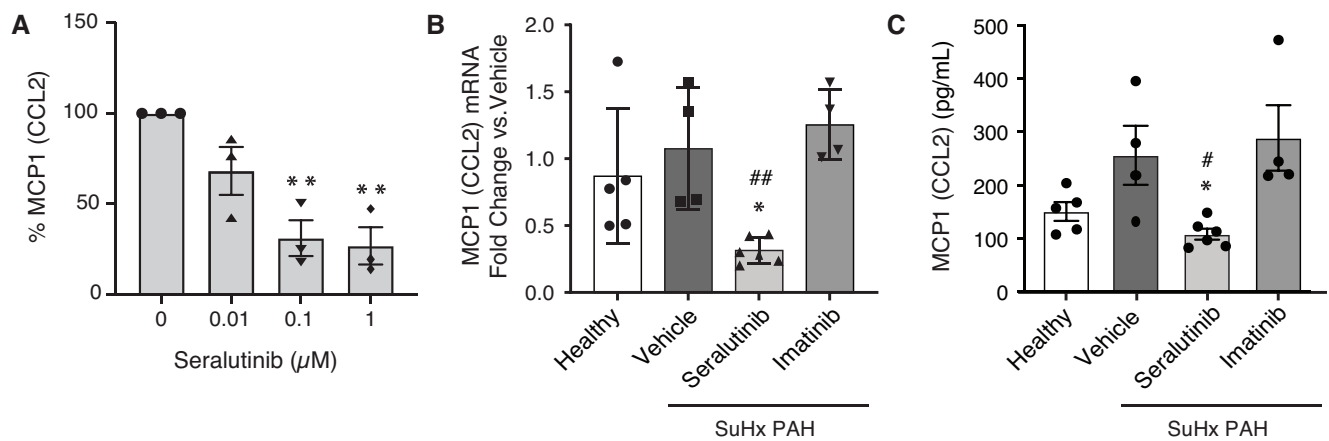


Figure S6. (A) Seralutinib effect on monocyte chemoattractant protein 1 (MCP-1/CCL2) secretion in primary human macrophages, determined after a 24-hour incubation with increasing concentrations of seralutinib. Data are shown as mean % expression relative to baseline \pm standard error of the mean (SEM) for $n=3$ independent donors. $**P<0.005$ versus vehicle. Impact of inhaled seralutinib or imatinib on monocyte chemoattractant protein 1 (MCP-1/CCL2) mRNA expression (B) or protein levels (C) in rat lungs from the SU5416/H pulmonary arterial hypertension (PAH) model at the end of treatment (Day 49, Study 3). Data are shown as mean \pm SEM for healthy ($n=4$), Vehicle ($n=4$), seralutinib ($n=6$) and imatinib ($n=4$). Statistical analysis performed using one-way analysis of variance (ANOVA) with Dunnett's (mRNA) or Tukey's (protein) Multiple Comparisons Test. $*P<0.05$ versus vehicle, $\#P<0.05$, $##P<0.01$ versus imatinib.

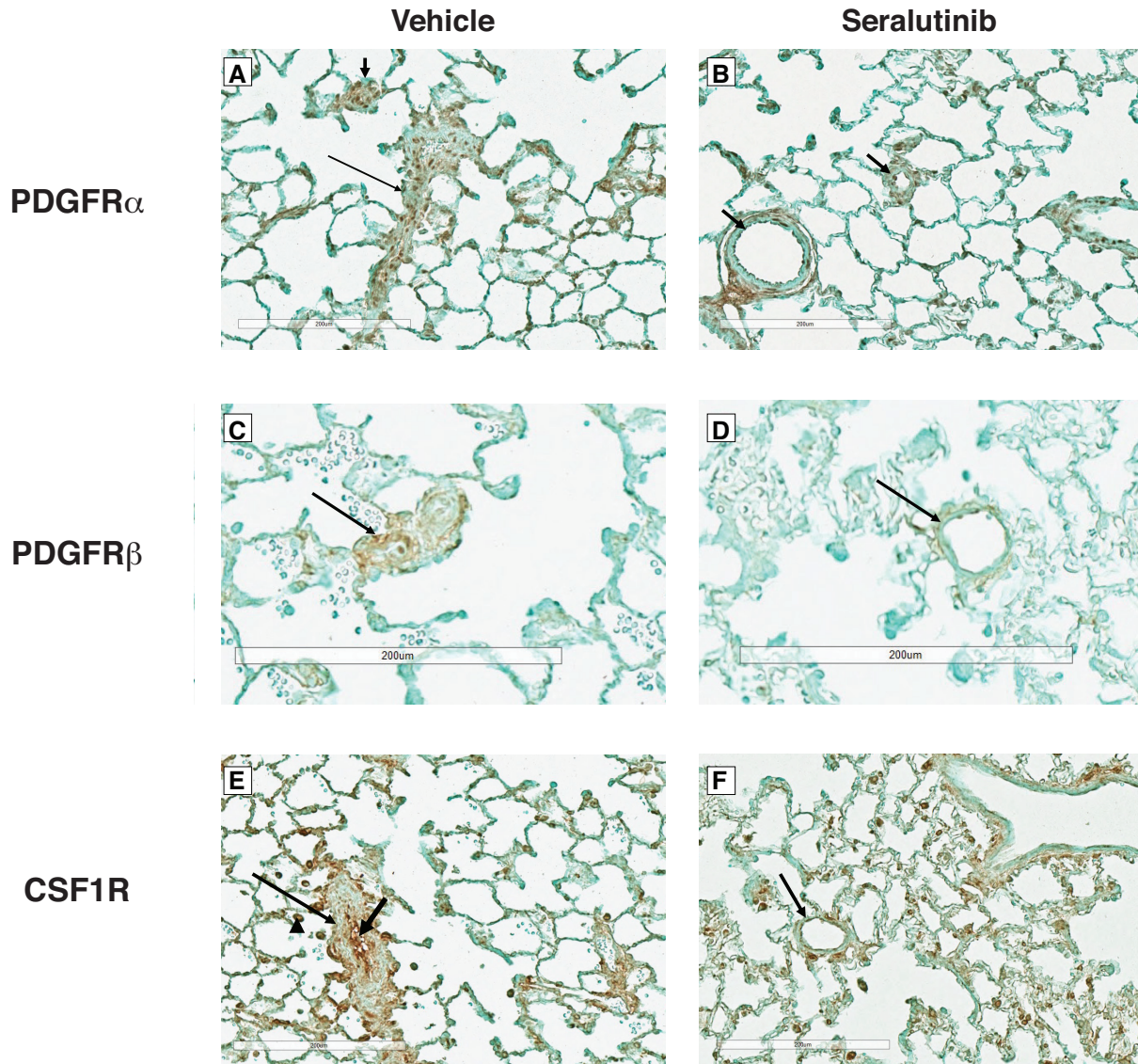


Figure S7. Representative lung tissue expression of PDGFR α (A-B), PDGFR β (C-D) and CSF1R (E-F) in vehicle- (A, C, E) and seralutinib- (B, D, F) treated SU5416/H rats. (A) Lung from SU5416/H vehicle-treated rat stained for PDGFR α . Pulmonary arterial vessels are seen both in long axis (long arrow) and short axis (short arrow). High signal for PDGFR α is seen mostly in the media, but also in the neointima. (B) Lung from SU5416/H seralutinib-treated rat showing patent small pulmonary arteries. PDGFR α is present but qualitatively decreased. Arrows point to small pulmonary arteries. (C) Lung from SU5416/H vehicle-treated rat stained for PDGFR β . (D) Lung from SU5416/H seralutinib-treated rat stained for PDGFR β . Arrows in C and D point to small pulmonary arteries. (E) Lung from SU5416/H vehicle-treated rat stained for CSF1R. Long arrow points to hypertrophied pulmonary artery. Short arrow points to neointima staining positive for CSF1R. Arrowhead points to an alveolar macrophage. (F) Lung from SU5416/H seralutinib-treated rat stained for CSF1R. Long arrow points to a small pulmonary artery.

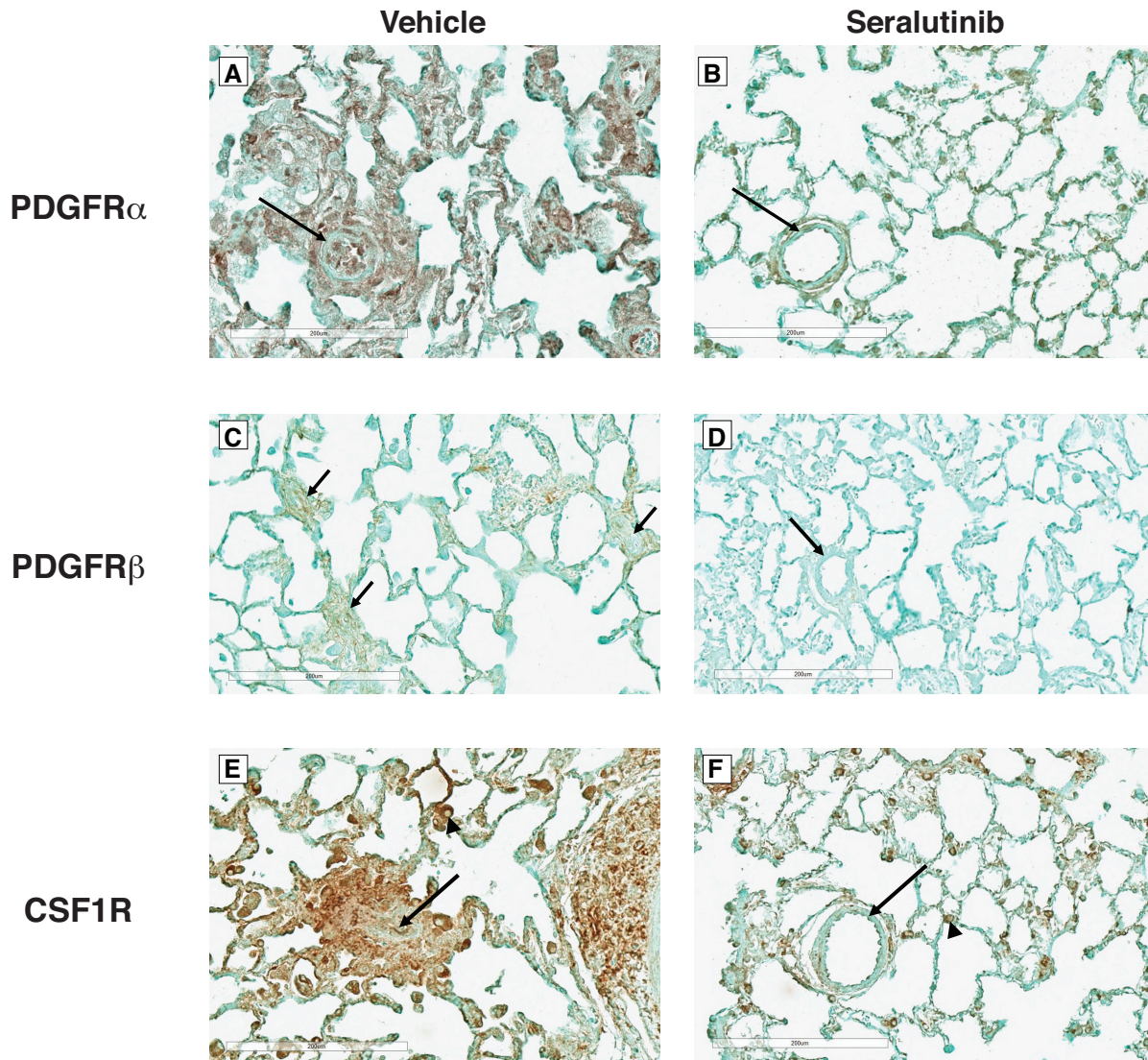


Figure S8. Representative lung tissue expression of PDGFR α (A-B), PDGFR β (C-D) and CSF1R (E-F) in vehicle- (A, C, E) and seralutinib- (B, D, F) treated MCTPN rats. (A) Lung from MCTPN vehicle-treated rat stained for PDGFR α . High signal is noted in the neointima and perivascular area of small pulmonary arteries. Arrow points to a small pulmonary artery. (B) Lung from MCTPN seralutinib-treated rat stained for PDGFR α . Arrow points to a small pulmonary artery. (C) Lung from MCTPN vehicle-treated rat stained for PDGFR β . Arrows point to small, essentially occluded, pulmonary arteries. Signal for PDGFR β is distributed throughout the lesions. (D) Lung from MCTPN seralutinib-treated rat stained for PDGFR β . Arrow points to a small pulmonary artery. There is very little signal for PDGFR β . (E) Lung from MCTPN vehicle-treated rat stained for CSF1R. There is intense perivascular signal. Arrow points to occluded lumen of a small pulmonary artery. (F) Lung from MCTPN seralutinib-treated rat stained for CSF1R. There is very little perivascular signal. Arrow points to a small pulmonary artery. Arrowheads in E and F point to alveolar macrophages.